ATOMS, MOLECULES, OPTICS

Electro- and Magneto-Optical Switching of Defect Modes in One-Dimensional Photonic Crystals

V. G. Arkhipkin[a,b], V. A. Gunyakov[a,b], S. A. Myslivets[a,b], V. Ya. Zyryanov[a,c], V. F. Shabanov[a,c], and Wei Lee[d]

[a]*Kirensky Institute of Physics, Krasnoyarsk Scientific Center, Russian Academy of Science, Siberian Branch, Krasnoyarsk, 660036 Russia*
[b]*Siberian Federal University, Krasnoyarsk, 660041 Russia*
[c]*Siberian State Aerospace University, Krasnoyarsk, 660014 Russia*
[d]*Department of Physics and Center for Nanotechnology, Chung Yuan Chistian University, Chung-Li, Taiwan, 32023, Republic of China*
e-mail: gun@iph.krasn.ru
Received May 25, 2010

Abstract—The transmission spectra of polarized light waves in a photonic crystal/liquid crystal (PC/LC) cell placed between crossed polarizers and controlled by an electric or magnetic field have been studied experimentally and theoretically. Electro- and magneto-optical switching based on the interference of polarized defect modes has been demonstrated. The transmission spectra of the PC/LC cell have been calculated as a function of the voltage applied to the LC layer and the magnetic field strength. The results of the calculations agree well with the experimental data.

1. INTRODUCTION

Photonic crystals (PCs) represent a wide class of materials with a spatial modulation of the refractive index with a period comparable to the light wavelength [1–3]. Such structures have photonic bandgaps in the transmission spectrum attributable to Bragg scattering (reflection). Breaking the periodicity gives rise to narrow transmission bands in the bandgaps called defect modes [1, 2]. They are localized in the defect region where the light wave intensity can exceed considerably the wave intensity at the PC exit. These PC properties allow the light fluxes to be efficiently controlled and have numerous applications in optoelectronics, laser physics and technology, photonics, and nonlinear optics [1, 3].

Multilayered periodic structures belong to the class of one-dimensional PCs. Such structures have long been investigated, but the approach based on the concept of PC allowed one to take a new look at their properties and to extend the possibilities for their application. For example, multilayered mirrors with a high reflectance in a wide frequency band almost at any angle of incidence for arbitrarily polarized light [4] and broadband filters with a transmission band independent of the angle of incidence [5] have been proposed. High-Q nanocavities [6, 7], low-threshold lasers [8], efficient nonlinear optical converters and optical parametric oscillators [9–11] have been produced on the basis of PCs with defects. Heterostructures with unique spectral characteristics (wide band-

gaps, large amplification of defect modes with a high Q factor) can be produced by combining PCs with various periods [12–14]. PCs also open new approaches for controlling the group velocity of light pulses [15, 16] and for writing, storing, and reading information [17].

PCs with a tunable resonance frequency are of particular interest. These structures are important for such applications as lasers, actively controlled filters, and all-optical switches. For these purposes, liquid crystals (LCs), which are included as structural elements, provide great possibilities [3, 18, 19]. Such LC properties as a wide transparency region, large optical birefringence, and strong nonlinearity as well as a high sensitivity to temperature, electric and magnetic fields [20] allow the PC properties to be efficiently controlled. Using LCs, one can continuously tune the bandgap position and the defect mode resonance frequency [3, 18], perform a high-speed defect mode switching (tens or hundreds of microseconds) [21], and control the light polarization. By now, the tuning of the PC/LC cell transmission and reflection spectra by an electric field [22–25], the temperature tuning [26], and the tuning through a change in the angle of incidence of light on PCs [19] have been realized. Recently, the possibility of an all-optical switch in a one-dimensional photonic crystal structure with a nematic LC defect has been proposed and realized using the light-induced orientational effect (the optical Freedericksz effect) [27, 28].

In this paper, we present the results of our experimental and theoretical studies of defect mode switching in a one-dimensional PC/LC cell placed between crossed polarizers by means of electric and magnetic fields. The electro- and magneto-optical interference amplification and quenching of defect modes with mutually orthogonal polarizations in the case of their spectral matching form the basis for switching. The essence of these phenomena consists in the following. When light passes through an optical cell that consists of two crossed polarizers and a plane-parallel film of optically uniaxial material between them, the interference of polarized light waves is observed [29]. The minimum intensity of transmitted light is reached under the condition

$$\frac{(n_e - n_o)L}{\lambda} = 0, 1, \ldots, k, \tag{1}$$

where n_e and n_o are the refractive indices of the uniaxial medium for the extraordinary and ordinary waves, respectively, L is the film thickness, and λ is the light wavelength in a vacuum. For the maximum intensity to be reached, the following relation must hold:

$$\frac{(n_e - n_o)L}{\lambda} = \frac{1}{2}, \frac{3}{2}, \ldots, k + \frac{1}{2}. \tag{2}$$

If a PC/LC cell is used instead of a plane-parallel film, then additional conditions for light transmission arise, because the defect modes in PC are formed when an integer number m of light half-wavelengths fits in the optical thickness of the defect layer. When an optically uniaxial material is used as the defect layer, the spectrum of defect modes is separated into two orthogonally polarized components for which the following conditions are met:

$$m_e \frac{\lambda_e}{2} = n_e L, \tag{3}$$

$$m_o \frac{\lambda_o}{2} = n_o L. \tag{4}$$

Here, the integer numbers $m_{e,o}$ denote the ordinal numbers of the defect modes. We see that in the case of spectral matching of the defect modes for the extraordinary and ordinary waves ($\lambda_e = \lambda_o = \lambda$), the difference of their ordinal numbers is defined by the relation

$$m_e - m_o = 2\frac{(n_e - n_o)L}{\lambda}. \tag{5}$$

Comparison of Eq. (5) with (1) and (2) shows that if the difference between the ordinal numbers of the polarized defect mode components is even, then a minimum intensity of transmitted light (destructive interference) is observed. If this quantity is odd, then the intensity of transmitted light is at a maximum (constructive interference). Spectral matching of the wavelengths of the ordinary and extraordinary waves can be achieved by means of an electric or magnetic field using the Freedericksz effect [20]. One can successively match the wavelengths of defect modes with

different indices and observe their quenching or amplification by varying the field strength. Note that the switching method under consideration differs from the previously suggested ones based on the defect mode peak shift (see, e.g., [30, 31].)

2. EXPERIMENTAL RESULTS

In this section, we present the results of our experimental studies of the transmission spectrum control for a one-dimensional PC/LC cell placed between crossed polarizers by means of electric and magnetic fields. The PC/LC cell consists of two identical multi-layered dielectric mirrors the gap between which is filled with a nematic LC. The mirrors consist of six zirconium dioxide (ZrO_2) layers and five silicon dioxide (SiO_2) layers alternately deposited on a fused silica substrate. The thicknesses of the ZrO_2 and SiO_2 layers are 55 and 102 nm, respectively. The refractive indices of ZrO_2 and SiO_2 are, respectively, 2.04 and 1.45 for $\lambda = 589$ nm.

The cell was located between crossed polarizers and was placed in an electric or magnetic field that was used to control the reorientation of LC molecules and, hence, the refractive indices. Electric and magnetic fields are known to lead to an orientational transition in a nematic LC called the Freedericksz effect [1, 20, 32]. Planar (for control by an electric field) and homeotropic (for a magnetic field) orientations of the nematic LC in the gap between the mirrors were used in our experiments. The S- and B-effects of electrically controlled birefringence are distinguished depending on the initial orientation of the field and the LC director $\mathbf{d}$ and on the sign of the nematic dielectric anisotropy $\Delta e = e_\parallel - e_\perp$ [20]. Here, the indices denote the LC permittivities parallel ($\parallel$) and perpendicular ($\perp$) to the director. S-deformation (S-effect) usually takes place for the initial planar orientation of the director and $\Delta e > 0$. B-deformation (B-effect) can take place for the initial homeotropic orientation of the director and $\Delta e < 0$ [20]. In both cases, the electric field is perpendicular to the LC layer. Analogs of these effects also exist in the case of control by an external magnetic field.

2.1. Defect Mode Switching in a PC/LC Cell by an Electric Field

The scheme of the electro-optical cell used in our experiments is shown in Fig. 1. It consists of two identical multilayered dielectric mirrors with the gap between them filled with a 5CB (4-n-pentil-4'-cyanobiphenyl) nematic LC and is placed between crossed polarizers. In the initial state, the LC director $\mathbf{d}$ has a planar orientation ($\mathbf{d} \parallel x$) with respect to the substrates. The thickness of the LC layer is 13.5 μm, the refractive indices of 5CB are $n_\parallel = 1.719$ and $n_\perp = 1.536$ ($T = 23°C$, $\lambda = 589$ nm) for light polarized, respectively, parallel and perpendicular to the director. A variable
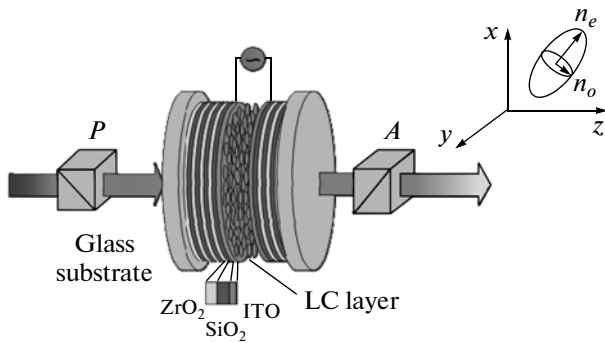
Fig. 1. Scheme of the electro-optical cell consisting of a one-dimensional PC/LC cells placed between crossed polarizers *P* and *A*. The voltage is applied to the defect layer. Also shown are the directions of the coordinate axes and the ellipsoid of the LC refractive index in an electric field.

Fig. 2. Transmission spectrum of the polarized components $T_\parallel$ ($\mathbf{P} \parallel x$, solid curve) and $T_\perp$ ($\mathbf{P} \parallel y$, dotted curve) for the PC/LC cell under study in the long-wavelength part of the bandgap.

electric field with a frequency of 800 Hz was applied to the ITO electrodes deposited over the dielectric multi-layers, making it possible to gradually reorient the nematic director by an angle up to 90° in the *xz* plane. In this case, the refractive index of the extraordinary (e) wave changes, while the refractive index of the ordinary (o) wave remains constant.

The transmission spectra of the optical cell were measured with a Shimadzu UV-3600 spectrometer for normally incident light. We used Glan prisms oriented at angles, respectively, β = ±45° to the *x* axis as polarizers *P* and *A* when performing our measurements in the geometry of crossed polarizers. In another variant, we used only the entrance polarizer *P* oriented either along the *x* axis or along the *y* axis to measure the polarized components of the transmission spectrum. A typical appearance of the polarized components in the transmission spectrum of the cell under study is presented in Fig. 2.

A number of defect modes are formed in the band-gap for both components. Nematic reorientation does not affect the ordinary component in the spectrum of defect modes and, at the same time, changes significantly the extraordinary component. In the case of $\mathbf{P} \parallel x$, a deviation of the director from the *x* axis causes the defect modes to be shifted to short wavelengths (Fig. 3). The spectrum insensitivity to low voltages applied to the defect layer, $U < U_c = 0.83$ V, is attributable to the threshold character of the Freedericksz transition.

Figure 4 shows the field dependences of the spectral positions of the defect mode peaks $\lambda_e(U)$ and $\lambda_o(U)$ for the extraordinary and ordinary waves, respectively. We see that the curves $\lambda_e(U)$ cross the horizontal lines $\lambda_o(U)$ corresponding to the ordinary component of the spectrum several times. Below, the crossing points will be called spectral matching of the polarized defect mode components. In this case, the necessary conditions for their interference at the exit from the analyzer
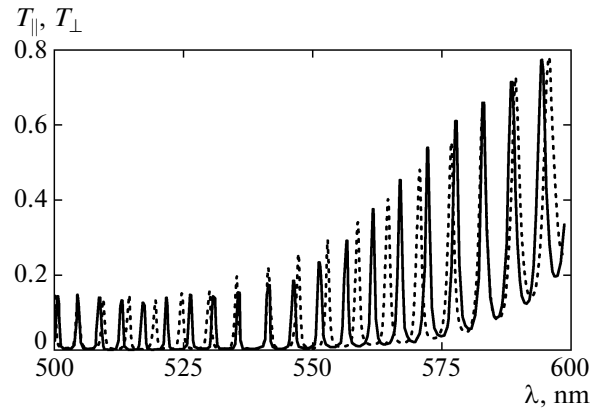
are fulfilled, which can be observed by measuring the intensity of the light passing through the optical cell. Generally, orthogonally polarized defect modes with the same wavelength have different ordinal numbers (Fig. 4). For example, as the field increases, the $\lambda_o = 584$ nm line (thick dashed line) corresponding to the 71st defect mode of the ordinary wave is alternately crossed by the defect modes of the extraordinary wave with the ordinal numbers 79, 78, 77, 76, etc. Only in the region where the nematic reorientation process is saturated does the 71st mode of the extraordinary component approach the 71st mode of the ordinary wave.
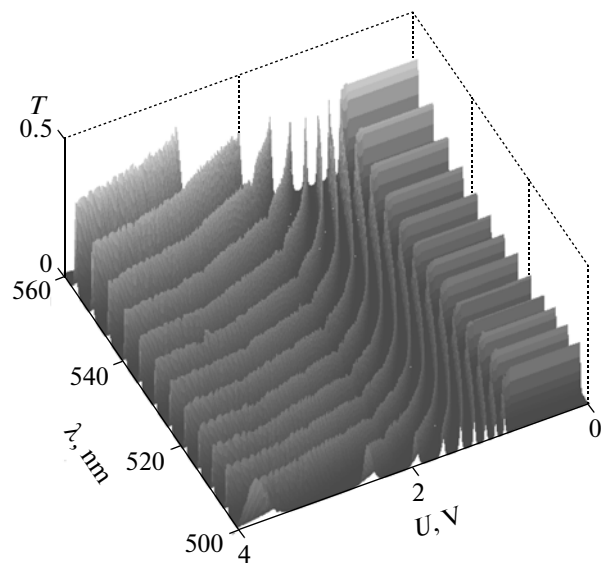
Fig. 3. Transformation of the spectrum of defect modes in the PC/LC cell for polarization $\mathbf{P} \parallel x$ when the director **d** is reoriented by an electric field (experiment).
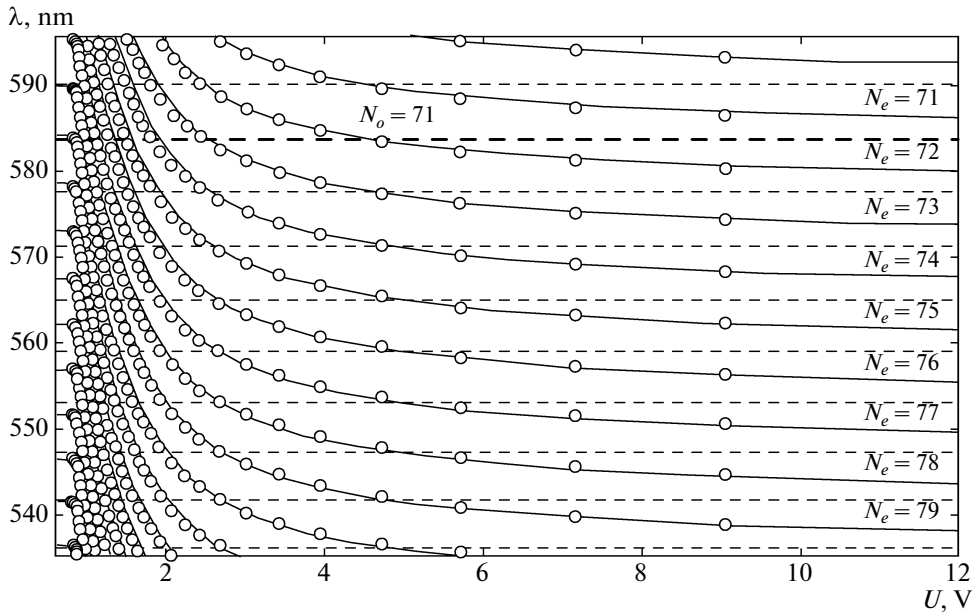
Fig. 4. Experimental (circles) and calculated (solid curves) field dependences of the spectral positions of the defect *e*-mode peaks in the PC/LC structure under study at long wavelengths. The dashed lines indicate the positions of the defect *o*-mode peaks.

Figure 5 shows the result of interference of the 79th and 78th modes of the extraordinary wave with the 71st mode of the ordinary component under the action of an electric field with $U_1 = 0.84$ V and $U_2 = 0.99$ V, respectively. As we see, if the difference between the ordinal numbers of the defect modes is even, then interference quenching of the transmitted light is observed. Conversely, if this difference is odd, then constructive interference takes place.

2.2. Defect Mode Switching in a PC/LC Cell by a Magnetic Field

The scheme of the experimental setup is shown in Fig. 6. The PC/LC cell is similar to that described in the preceding section. The gap between the mirrors is filled with a 4-methoxybenzylidene–4'-butylaniline (MBBA) nematic LC. In the initial state, the LC director **d** is oriented homeotropically with respect to the substrates (**d** ‖ *z*). To produce a homeotropically oriented LC sample, the mirror surface was treated with a 0.6% alcoholic solution of lecithin. The thickness of the LC layer is $L = 13.8$ μm; the refractive indices of MBBA are $n_e = 1.765$ and $n_o = 1.552$ ($T = 26°C$, $\lambda = 589$ nm) for light polarized parallel and perpendicular to the director.

The PC/LC cell was placed in the field of a stationary FEL magnet (20 kOe, **H** ‖ *x*), which made it possible to gradually reorient the nematic director by an angle up to 90° in the *xz* plane with increasing magnetic field strength. At $H > H_c$, the polarized components of the defect modes are split. As *H* increases, the effective refractive index of the extraordinary wave $\langle n_e \rangle$ changes from n_o for **d** ‖ *z* to n_e for **d** ‖ *x*, while the refractive index of the ordinary wave n_o remains constant. The transmission spectra of the PC/LC cell were measured with an Ocean Optics HR4000 spectrometer. Optical fibers were used for the input of light into the sample and for its output to the spectrometer. We used Glan prisms oriented, respectively, at $\beta = \pm45°$ to the *x* axis as polarizers *P* and *A* when performing our mea-
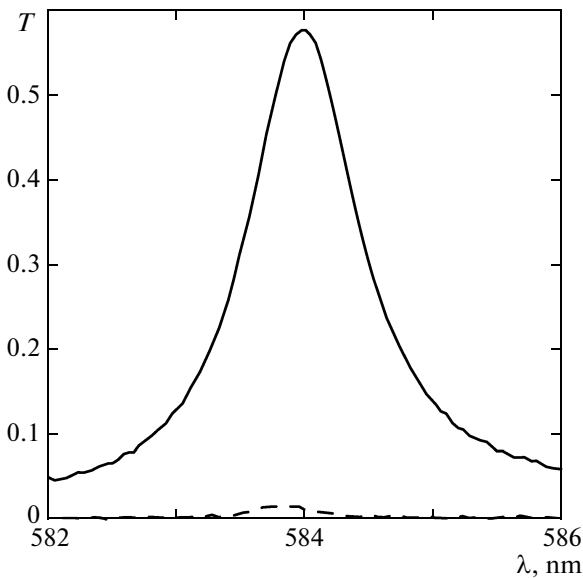
Fig. 5. Light transmission of the optical cell shown in Fig. 1 in the case of interference of the 79th ($U_1 = 0.84$ V, dashed curve) and 78th ($U_2 = 0.99$ V, solid curve) extraordinary modes with the 71st ordinary mode.
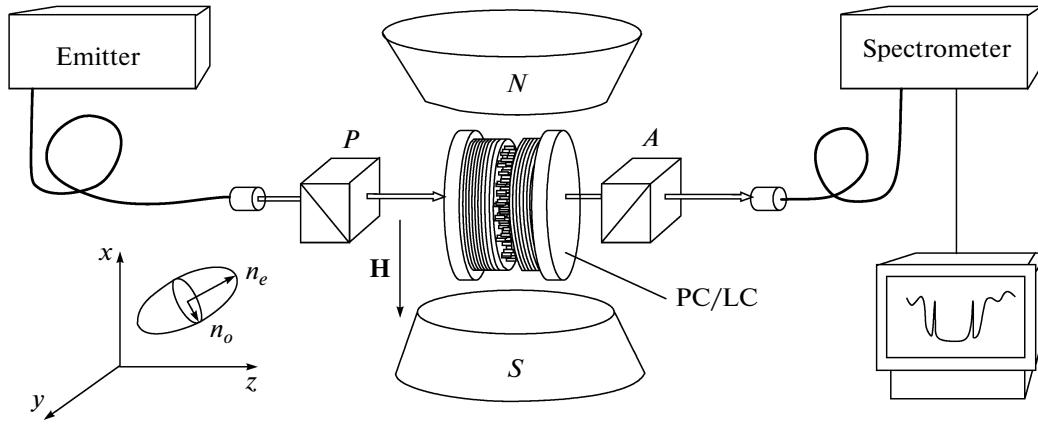
Fig. 6. Scheme of the magneto-optical setup to investigate the light transmission of a one-dimensional PC/LC cell placed between crossed polarizers.

surements in the geometry of crosses polarizers. The polarized components of the transmission spectra were measured only with the entrance polarizer *P* oriented either along the *x* axis or along the *y* axis.

Figure 7 shows the experimental dependences of the spectral positions of the defect mode peaks on magnetic field strength (circles). Here, the Freedericksz threshold field is $H_c = 6.3$ kOe. According to Eqs. (3) and (4), the defect mode spectrum above the Freedericksz threshold H_c is separated into two independent orthogonally polarized components with wavelengths

$$\lambda_e = \frac{2Ln_e}{m_e}, \quad \mathbf{P} \parallel x \qquad (6a)$$

for the *e*-mode and

$$\lambda_o = \frac{2Ln_o}{m_o}, \quad \mathbf{P} \parallel y \qquad (6b)$$

for the *o*-mode. As the magnetic field increases, the *e*-mode wavelength is shifted long wavelengths. We see that any horizontal $\lambda_o = \text{const}$ line with number m_o above the Freedericksz threshold has several crossings with the curves of the spectral positions of the *e*-mode peaks $\lambda_e(H)$ with numbers $m_e = m_o + 1, m_o + 2, ...,$ etc. The crossing points of the curves correspond to the spectral matching $\lambda_e = \lambda_o$ of the orthogonally polarized modes. In this case, if the PC/LC cell is placed between crossed polarizers, then their interference can be observed. As has been noted in the Introduction, the intensity of transmitted light depends on the difference between the ordinal defect mode numbers $m_e - m_o$.

Figure 8 presents the experimental dependence of the light transmission for a PC/LC cell placed between crossed polarizers on wavelength and reduced magnetic field. The spectra were recorded with a 0.02-kOe step at fixed temperature $(23.0 \pm 0.5)°C$. Below the Freedericksz threshold, $H < H_c$, the light transmission is nearly zero in the entire spectrum. This is because

degeneracy of the *e*- and *o*-modes with the same ordinal number $(m_e = m_o)$ takes place and, according to (5), the intensity of transmitted light is at a minimum. At $H \geq H_c$, degeneracy is removed, but the modes are not yet spectrally resolved due to their finite width $(\delta\lambda \approx 2$ nm). As the field increases further, both transmission components are seen separately. One of them (*o*-mode) is left in place, while the second (*e*-mode) is shifted to long wavelengths. At $\lambda_e = \lambda_o$, there is interference between these components, which leads to an alternation of transmission maxima and minima in the
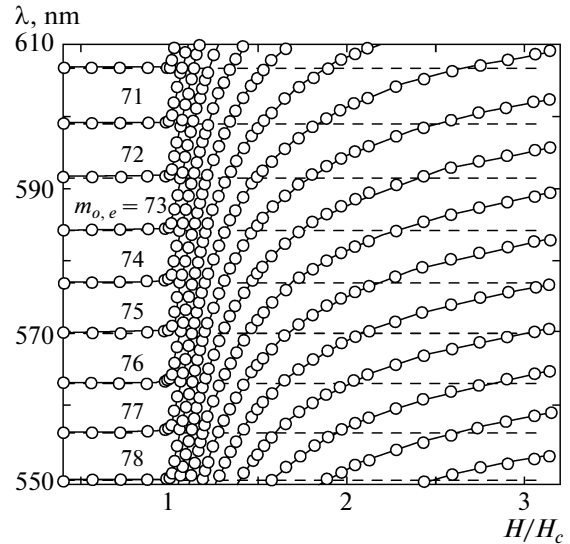
Fig. 7. Field dependences of the spectral positions of the *e*-mode peaks in the PC/LC cell: the circles and solid lines represent the experimental data and the results of our calculations by the recurrence method, respectively. The dashed lines indicate the positions of the *o*-mode peaks. The temperature is 23°C, the thickness of the LC layer is $L = 13.8$ μm, and the threshold field is $H_c = 6.3$ kOe.
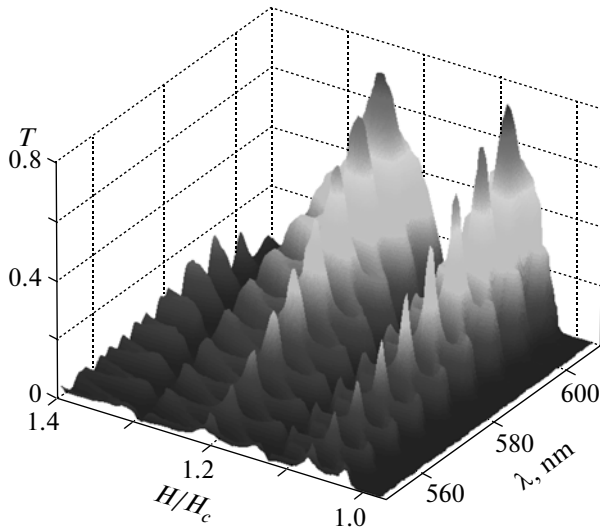
Fig. 8. Experimental dependence of the light transmission of a PC/LC cell placed between crossed polarizers on wavelength and reduced magnetic field, $H_c = 6.3$ kOe.
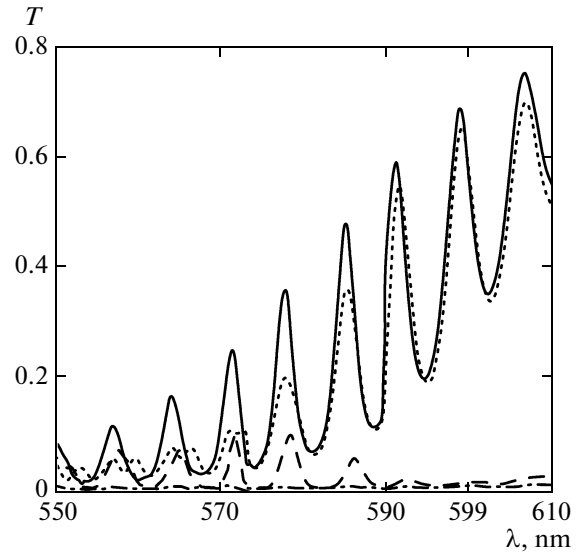

Fig. 9. Magneto-optical switching of the PC/LC cell spectrum. The dash−dotted curve indicates the transmission at a field strength $H < H_c$; the solid line correspond to the first defect mode intensity maximum at $H/H_c = 1.073$, the dashed curve corresponds to the first minimum at $H/H_c = 1.147$, and the dotted curve is the second maximum at $H/H_c = 1.232$. All lines correspond to the extrema at $\lambda_o = 599$ nm.

direction of the coordinate H in accordance with the selection rules (1)−(5).

Note that the modulation of light transmission observed in Fig. 8 is coherent in character. Indeed, as the director **d** is reoriented and as the effective nematic refractive index grows,

$$\langle n_e \rangle = \frac{1}{L} \int_0^L n(z) dz \longrightarrow n_e,$$

two differently directed trends determining the behavior of e-modes in various parts of the photonic bandgap above the Freedericksz threshold manifest themselves. On the one hand, all e-modes are redshifted relative to the static set of o-modes. On the other hand, in view of the relation $\Delta\lambda = \lambda^2/2Ln$ known from the theory of a Fabry−Perot interferometer [33], the intermode spacing $\Delta\lambda_e$ decreases. Since the starting position of the e-modes is specified by the position of the corresponding o-modes, the simultaneous action of these factors will lead to a monotonic slowdown of the mode shift in the direction from the short-wavelength bandgap edge to the long-wavelength one. As a result, a gradual increase in the field strength will lead to a successive switch-on (switch-off) of the light transmission peaks.

For PC structures whose spectrum is characterized by a small intermode spacing $\Delta\lambda$, it turns out to be possible to get a quasi-synchronous switch-on of modes in a limited interval of the bandgap. Such a situation was realized for the PC/LC structure under study in the wavelength range 550−610 nm at a field strength $H/H_c = 1.07$ that slightly exceeds the threshold value of $H_c = 6.3$ kOe and corresponds to the first mode crossing (Fig. 9).

In the case under consideration, the change in the spacing between neighboring modes does not exceed their spectral width and the modes are switched on almost simultaneously (solid line). As the field increases, a successive switch-on of modes will be observed. Indeed, at $H/H_c = 1.232$ corresponding to the third crossing of the chosen $\lambda = 599$ nm mode, maximum transmission is observed only for this mode (dotted line). We see from the figure that the profiles of the shorter-wavelength modes begin to split up and have already passed the maximum transmission, while the longer-wavelength modes have not yet reached it. Note that not only the modes but also, in contrast to the switching methods based on the mode shift [30, 31], the background level are switched off in the T_{off} state. This leads to a significant increase in the contrast ratio.

Deforming the LC by an external magnetic field, we can obtain the dependence of the light transmission at fixed wavelength corresponding to any o-mode. Figure 10 presents a typical field dependence of the transmission $T(H)$ for the PC structure under study at $\lambda_o = 591.9$ nm. We see from the plot that the conditions for maxima and minima are fulfilled several times. The first maximum ($H/H_c = 1.073$), first minimum ($H/H_c = 1.143$), and second maximum ($H/H_c = 1.227$) correspond to the first, second, and third mode crossings, respectively. The "shoulders" observed on both sides of the maxima roughly correspond to the transmission level of the o-mode nonoverlapping with the e-modes. To switch the PC/LC cell from the
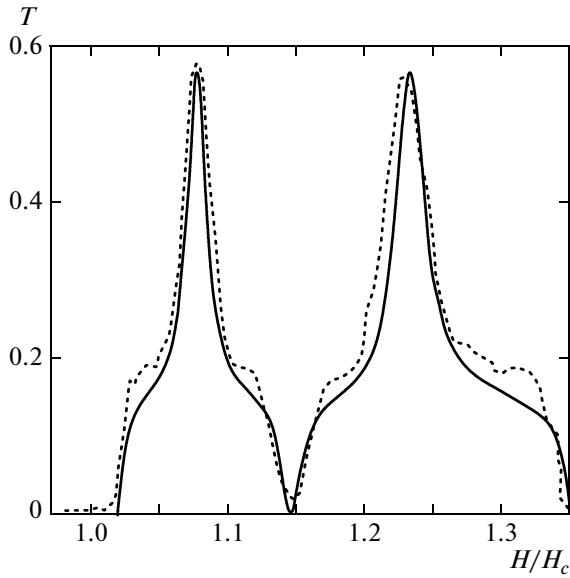
Fig. 10. Experimental (dotted) and calculated (solid curve) light transmission modulation curves for the PC/LC cell at a wavelength of 591.9 nm.

closed state (T_{off}) state to the first transparent one (T_{on}), the field should be changed by 0.4 kOe.

3. MODELING THE LIGHT TRANSMISSION OF SWITCHED PHOTONIC CRYSTALS AND DISCUSSION OF EXPERIMENTAL RESULTS

3.1. PC/LC Cell in a Magnetic Field

Let us first consider the case of switching by a magnetic field. The PC under study is a layered $(HL)^N H(D)H(LH)^N$-type structure, as shown in Fig. 11. Here, the letters H and L denote the various dielectric, optically isotropic layers with high (H) and low (L) refractive indices n_1 and n_2 and thicknesses t_1 and t_2, respectively; the lattice period is $t = t_1 + t_2$; D is the defect layer with a refractive index n_d and thickness t_d; and N is the number of HL and LH bilayers (periods). The defect layer is filled with a homeotropically oriented nematic LC. We will assume that the structure under consideration is bounded by a vacuum ($n = 1$) at the left and the right and that a plane monochro-

matic light wave is normally incident on the PC from the left. The crystal is placed in a stationary magnetic field H perpendicular to the PC optical z axis (Fig. 6).

In the initial state in the laboratory frame at $H < H_c$, the LC permittivity tensor is

$$\varepsilon(\lambda) = \begin{pmatrix} \varepsilon_\perp & 0 & 0 \\ 0 & \varepsilon_\perp & 0 \\ 0 & 0 & \varepsilon_\parallel \end{pmatrix},$$

where $\varepsilon_\perp = n_\perp^2 = n_o^2$ and $\varepsilon_\parallel = n_\parallel^2 = n_e^2$ are the permittivity components perpendicular and parallel to the director, respectively.

As long as the magnetic field strength H is less than the critical one H_c, it does not affect the transmission spectrum of the PC/LC cell. At $H > H_c$, the LC director turns in the xz plane, causing the permittivity tensor to change. It takes the form

$$\varepsilon(\lambda) = \begin{pmatrix} \varepsilon_{xx} & 0 & \varepsilon_{xz} \\ 0 & \varepsilon_{yy} & 0 \\ \varepsilon_{zx} & 0 & \varepsilon_{zz} \end{pmatrix}$$

$$= \begin{pmatrix} \varepsilon_\perp \cos^2\theta + \varepsilon_\parallel \sin^2\theta & 0 & \Delta\varepsilon \cos\theta \sin\theta \\ 0 & \varepsilon_\perp & 0 \\ \Delta\varepsilon \cos\theta \sin\theta & 0 & \varepsilon_\perp \sin^2\theta + \varepsilon_\parallel \cos^2\theta \end{pmatrix},$$

where $\Delta\varepsilon = \varepsilon_\parallel - \varepsilon_\perp = n_e^2 - n_o^2$ is the optical dielectric anisotropy and $\theta \equiv \theta(z)$ is the angle between the z axis and the local direction of the director **d**.
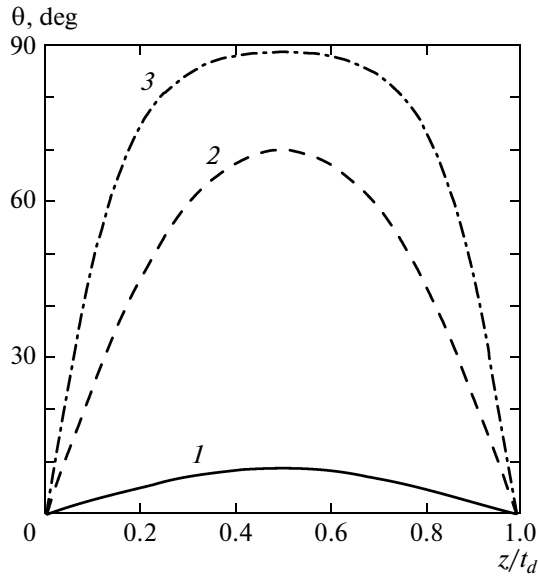
The local refractive index for the extraordinary wave in the LC layer is uniquely related to the angle θ for an arbitrary orientation of the LC director with respect to the magnetic field vector (or the x axis) [29]:

$$n(z) = \frac{n_e n_o}{\sqrt{n_e^2 \cos^2\theta(z) + n_o^2 \sin^2\theta(z)}}. \quad (7)$$

The angle θ is calculated by minimizing the free energy density. For the B-effect in a magnetic field, the
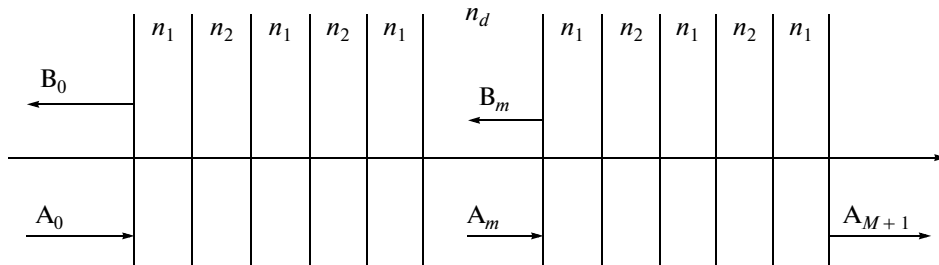
Fig. 11. Schematic view of a one-dimensional PC structure with an LC layer as a defect.

Fig. 12. Calculated distributions of the orientation angle $\theta(z)$ for the nematic director of a deformed LC inside the defect layer of a PC cell for various magnetic field strengths: $H/H_c = 1.01$ (*1*), 1.5 (*2*), and 3.0 (*3*).
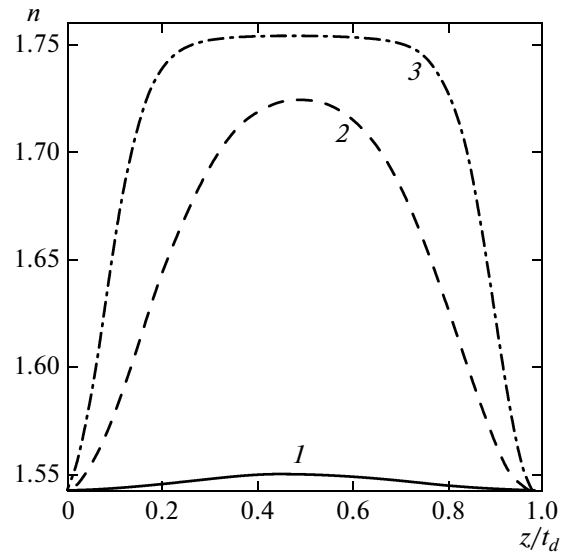
Fig. 13. Refractive index for the extraordinary wave in MBBA versus normalized coordinate for various magnetic field strengths: $H/H_c = 1.01$ (*1*), 1.5 (*2*), and 3.0 (*3*).

free energy per unit volume of an LC layer enclosed between two solid surfaces is [20]

$$F = \frac{1}{2}(k_{11}\cos^2\theta + k_{33}\sin^2\theta)\left(\frac{d\theta}{dz}\right)^2 - \frac{1}{2}\chi_a H^2\cos^2\theta,$$

where k_{11} and k_{33} are the elastic constants of the splay and bend deformations, χ_a is the diamagnetic anisotropy.

The minimization procedure leads to the equation

$$(k_{11}\cos^2\theta + k_{33}\sin^2\theta)\frac{d^2\theta}{dz^2} + \frac{k_{33} - k_{11}}{2}$$

$$\times \sin(2\theta)\left(\frac{d\theta}{dz}\right)^2 + \frac{1}{2}\chi_a H^2\sin(2\theta) = 0. \tag{8}$$

Equation (8) is solved numerically with the boundary conditions $\theta(0) = \theta(L) = 0$ and $k_{11} = 6$ pN, $k_{33} = 7.5$ pN [34], and $\chi_a = 0.97 \times 10^{-7}$ [35] taken for an MBBA nematic LC at a temperature of 25°C. For our numerical calculations, we used the parameters give above (Sect. 2) in the description of the experiment.

Figure 12 shows the distribution of the angle $\theta(z)$ in a defect layer containing MBBA for several magnetic field strengths calculated using Eq. (8). Using the calculated distribution $\theta(z)$, we derived the dependence of the refractive index for the extraordinary wave on normalized coordinate for various magnetic field strengths based on Eq. (7) (Fig. 13). The refractive index has a nonuniform distribution inside the defect layer and depends strongly on the applied magnetic field.

To calculate the transmission spectra, we used the method of recurrence relations [19, 36]. All layers were divided into a number M of sublayers large enough for the refractive index in each of them to be considered

constant. The field in an arbitrary sublayer m can be represented as a superposition of forward and backward waves traveling toward each other:

$$E_m(z) = A_m\exp[ik_m(z - z_m)]$$

$$+ B_m\exp[-ik_m(z - z_m)], \tag{9}$$

where $k_m = 2\pi n_m/\lambda$, n_m is the refractive index of the corresponding sublayer.

The amplitudes A_m and B_m are calculated from the recurrence relations [19]

$$A_{m+1} = A_m\frac{1 + R_m}{g_{m+1}^{-1} + g_{m+1}R_{m+1}},$$

$$B_m = R_m A_m, \tag{10}$$

$$R_m = \frac{r_m + g_{m+1}^2 R_{m+1}}{1 + r_m g_{m+1}^2 R_{m+1}},$$

where

$$g_m = \exp(ik_m t_m), \quad t_m = z_{m+1} - z_m,$$

$$r_m = \frac{k_m - k_{m+1}}{k_m + k_{m+1}}.$$

The transmission and reflection coefficients are defined by the relations

$$T = \left|\frac{A_{M+1}}{A_0}\right|^2, \quad R = \left|\frac{B_0}{A_0}\right|^2. \tag{11}$$

Here, A_0 and B_0 are the amplitudes of the forward and reflected waves at the PC entrance, A_{M+1} is the amplitude of the forward wave at the PC output.

The solid lines in Fig. 7 indicate the calculated dependences of the spectral positions of the defect

mode peaks on magnetic field strength, which show good agreement with the experiment. The calculated dependence of the transmission on magnetic field strength for a given wavelength (Fig. 10) also agrees satisfactorily with the experimental curve. In our calculations, we took into account the damping of defect modes due to the losses in the PC [19].

3.2. PC/LC Cell in an Electric Field

The defect mode switching in an electric field is similar to the case with a magnetic field considered. However, it is more difficult to analyze theoretically. The reason is that the magnetic field in the defect layer is uniform, while the electric field is distributed nonuniformly, because the LC static permittivity e depends on the coordinate along the PC z axis (Fig. 1). However, this peculiarity is not always taken into account when photonic crystals with an LC defect are investigated.

In the initial state in the laboratory frame at $U < U_c$, the LC permittivity tensor at optical frequencies is

$$\varepsilon(\lambda) = \begin{pmatrix} \varepsilon_\| & 0 & 0 \\ 0 & \varepsilon_\perp & 0 \\ 0 & 0 & \varepsilon_\perp \end{pmatrix}.$$

As long as the voltage on the electrodes between which the LC is located is less than the critical one U_c, the electric field does not affect the transmission spectrum of the PC/LC cell. At voltages $U > U_c$, the LC director turns in the xz plane, causing the permittivity tensor to change:

$$\varepsilon(\lambda) = \begin{pmatrix} \varepsilon_\perp \sin^2\theta + \varepsilon_\| \cos^2\theta & 0 & \Delta\varepsilon\cos\theta\sin\theta \\ 0 & \varepsilon_\perp & 0 \\ \Delta\varepsilon\cos\theta\sin\theta & 0 & \varepsilon_\perp\cos^2\theta + \varepsilon_\|\sin^2\theta \end{pmatrix}.$$

Accordingly, the expression for the refractive index takes the form

$$n(z) = \frac{n_e n_o}{\sqrt{n_e^2 \sin^2\theta(z) + n_o^2\cos^2\theta(z)}}, \qquad (12)$$

where θ is the angle between the x axis and the local direction of the director $\mathbf{d}(z)$.

The angle θ is calculated by minimizing the free energy density. For the S-effect in an electric field, the free energy per unit volume of a LC layer enclosed between two solid surfaces is [37]

$$F = \frac{1}{2}(k_{11}\cos^2\theta + k_{33}\sin^2\theta)\left(\frac{d\theta}{dz}\right)^2 - \frac{1}{2}(\mathbf{D}\cdot\mathbf{E}).$$

In this case, the equation defining the orientation angle of the LC director θ in an electric field takes the form

$$(k_{11}\cos^2\theta + k_{33}\sin^2\theta)\frac{d^2\theta}{dz^2} + \frac{k_{33} - k_{11}}{2}\sin(2\theta)$$

$$\times \left(\frac{d\theta}{dz}\right)^2 + \frac{D_z^2}{2\varepsilon_0}\frac{(e_\| - e_\perp)\sin(2\theta)}{(e_\perp\sin^2\theta + e_\|\cos^2\theta)^2} = 0. \qquad (13)$$

Here,

$$D_z = \varepsilon_0 U\left\{\int_0^L \frac{dz}{e_\perp\sin^2\theta + e_\|\cos^2\theta}\right\}^{-1}$$

is the component of the electric displacement vector in the defect layer along the z axis and U is the voltage applied to the LC layer. Equation (13) is solved under the boundary conditions $\theta(0) = \theta(L) = 0$ with the 5CB nematic material constants $k_{11} = 7.3$ pN, $k_{33} = 10.3$ pN, $e_\perp = 6$, and $e_\| = 18$ [35] taken at a temperature of 23°C.

Figure 14 presents the results of our calculations of the 5CB refractive index in the defect layer as a function of coordinate performed both with a nonuniform electric field distribution inside the defect and under the assumption of its uniformity. We see that when the Freedericksz threshold is exceeded considerably $U \geq 5U_c$), the distributions of the refractive index essentially coincide. Otherwise, the nonuniformity of the field distribution should be taken into account.

The dependences of the spectral positions of the defect mode peaks on applied voltage U calculated using Eqs. (9)–(11) are presented in Fig. 4 (solid lines). As we see, the results of our calculations show good agreement with the experimental data.

Figure 15 presents the calculated dependences of the light transmission for a PC/LC cell placed between crossed polarizers on wavelength and applied voltage. In contrast to the B-effect (see Fig. 8), both o- and e-components are observed in the transmission spectrum below the Freedericksz threshold $U < U_c$. Above the threshold ($U > U_c$), an alternation of maxima and minima attributable to the interference of o- and e-modes in the case of their spectral matching according to the selection rules (1)–(5) is observed in the transmission spectrum.

4. CONCLUSIONS

The transmission spectra of polarized light waves in a PC/LC cell placed between crossed polarizers and controlled by external electric and magnetic fields were studied experimentally and theoretically. Transmission spectrum switching based on the interference of polarized components, which leads to an oscillating field dependence of the PC/LC cell light transmission, was demonstrated. Both interference amplification and quenching of the light intensity can take place at the exit from the optical system in the case of spectral matching of orthogonally polarized defect modes,
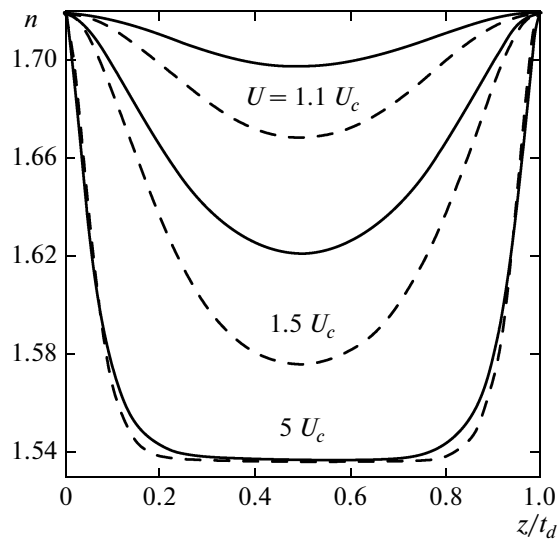
Fig. 14. Distributions of the refractive index $n(z)$ for a 5CB nematic in a PC defect calculated for various voltages with (solid curves) and without (dashed curves) allowance for the spatial electric field nonuniformity.
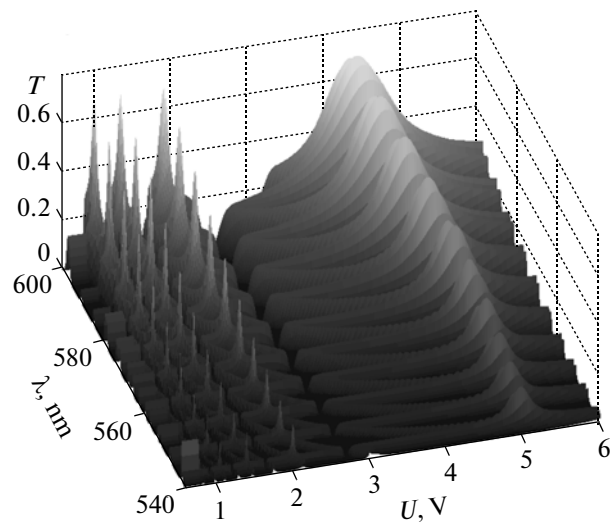
Fig. 15. Dependence of the light transmission of a PC/LC cell placed between crossed polarizers on wavelength and voltage.

depending on the difference between the ordinal defect mode numbers.

Our studies of the spectral properties of a multilayered PC/LC structure during orientational transitions of a nematic defect layer revealed a number of features attributable to the specificity of the applied geometry of crossed polarizers. We showed that the oscillating field dependence of the PC/LC cell light transmission is coherent. The behavior of the extraordinary defect modes in the spectrum is affected by differently directed trends related to the change in the effective refractive index of the LC medium when the director is reoriented. We established that for PC structures with a small intermode spacing in the spectrum, the cell can be switched from an optically closed state in a wide spectral range to a state with synchronously open spectral transparency windows. In addition, the light transmission of the PC/LC cell was modulated at the frequencies of ordinary defect modes by periodically alternating the parity of the ordinal numbers of combining defect modes. Based on the method of recurrence relations, we performed a numerical analysis of the transmission spectra and modulation curves for the PC structure under study, which showed good agreement with the experimental data. It should be noted that the magnetic field was used only to test an alternative field action. Such results can be obtained if an electric field is applied instead of a magnetic field to reorient a homeotropically oriented nematic layer.

ACKNOWLEDGMENTS

REFERENCES

1. V. F. Shabanov, S. Ya. Vetrov, and A. V. Shabanov, *Optics of Real Photonic Crystals: Liquid-Crystal Defects and Inhomogeneities* (Siberian Branch of the Russian Academy of Sciences, Novosibirsk, 2005) [in Russian].

2. K. Busch, G. von Freymann, S. Linden, S. F. Mingaleev, L. Tkeshelashvili, and M. Wegener, Phys. Rep. **444**, 101 (2007).

3. E. Ozbay, I. Bulu, K. Aydin, H. Gaglayan, and K. Guven, Photonics Nanostruct. **2**, 87 (2004).

4. Y. Fink, J. N. Winn, S. Fan, C. Chen, J. Michel, J. D. Joannopoulos, and E. L. Thomas, Science (Washington) **282**, 1679 (1998).

5. A. Mandatori, S. Sibilia, M. Bertolotti, S. V. Zhukovsky, and S. V. Gaponenko, J. Opt. Soc. Am. B **22**, 1785 (2005).

6. P. Lannane, C. Sauvan, and J. Hugonin, Laser Photonics Rev. **2**, 514 (2008).

7. D. Englund, H. Altug, B. Ellis, and J. Vučković, Laser Photonics Rev. **2**, 264 (2008).

8. K. Nozaki, S. Kita, and T. Baba, Opt. Express **15**, 7506 (2007).

9. B. Shi, Z. V. Jiang, and X. Wang, Opt. Lett. **26**, 1194 (2001).

10. F. Wang, S. N. Zhu, K. F. Li, and K. W. Cheah, Appl. Phys. Lett. **88**, 071 102 (2006).

11. F.-F. Ren, R. Li, C. Cheng, J. Chen, Y.-X. Fan, J. Ding, and H.-T. Wang, Phys. Rev. B: Condens. Matter **73**, 033 104 (2006).

12. G. Liang, P. Han, and H. Wang, Opt. Lett. **29**, 192 (2004).

13. Y.-H. Chang, C.-C. Liu, T.-J. Yang, and C.-J. Wu, J. Opt. Soc. Am. B **26**, 1141 (2009).

14. Z. Wang, L. Wang, Y. Wu, L. Chen, X. Chen, and W. Lu, Appl. Phys. Lett. **84**, 1629 (2004).

15. V. G. Arkhipin and S. A. Myslivets, Kvantovaya Elektron. (Moscow) **39**, 157 (2009).

16. V. G. Arkhipin and S. A. Myslivets, Phys. Rev. A: At., Mol., Opt. Phys. **80**, 061 802(R) (2009).

17. Z. S. Yang, N. H. Kwong, R. Binder, and A. L. Smirl, J. Opt. Soc. Am. B **22**, 2144 (2002).

18. H. Kitzerow, Liq. Cryst. Today **11**, 3 (2002).

19. V. G. Arkhipin, V. A. Gunyakov, S. A. Myslivets, V. P. Gerasimov, V. Ya. Zyryanov, S. Ya. Vetrov, and V. F. Shabanov, Zh. Eksp. Teor. Fiz. **133** (2), 447 (2008) [JETP **106** (2), 388 (2008)].

20. L. M. Blinov, *Electro-Optical and Magneto-Optical Properties of Liquid Crystals* (Nauka, Moscow, 1978; Wiley, New York, 1983).

21. R. Ozaki, H. Moritaki, K. Yoshino, and M. Ozaki, J. Appl. Phys. **101**, 033 503 (2007).

22. R. Ozaki, T. Matsui, M. Ozaki, and K. Yoshino, Jpn. J. Appl. Phys., Part 2 **41**, L1482 (2002).

23. S. M. Weiss, H. Ouyang, J. Zhang, and Ph. Fauchet, Opt. Express **13**, 1090 (2005).

24. S. M. Weiss and Ph. M. Fauchet, Phys. Status Solidi A **197**, 556 (2003).

25. V. Ya. Zyryanov, V. A. Gunyakov, S. A. Myslivets, V. G. Arkhipin, and V. F. Shabanov, Mol. Cryst. Liq. Cryst. **488**, 118 (2008).

26. V. A. Gunyakov, V. P. Gerasimov, S. A. Myslivets, V. G. Arkhipin, S. Ya. Vetrov, G. N. Kamaev, A. V. Sha-banov, V. Ya. Zyryanov, and V. F. Shabanov, Pis'ma Zh. Tekh. Fiz. **32** (21), 76 (2006) [Tech. Phys. Lett. **32** (11), 951 (2006)].

27. A. Miroshnichenko, I. Pinkevych, and Yu. S. Kivshar, Opt. Express **14**, 2839 (2006).

28. U. A. Laudyn, A. Miroshnichenko, W. Krolikowski, D. F. Chen, Y. S. Kivshar, and M. A. Karpierz, Appl. Phys. Lett. **92**, 203 304 (2008).

29. S. A. Akhmanov and S. Yu. Nikitin, *Physical Optics* (Oxford University Press, Oxford, 1997; Moscow State University, Moscow, 1998).

30. R. Ozaki, H. Moritaki, K. Yoshino, and M. Ozaki, J. Appl. Phys. **101**, 033 503 (2007).

31. R. Ozaki, M. Ozaki, T. Matsui, and K. Yoshino, Jpn. J. Appl. Phys., Part 2 **41**, L1482 (2002).

32. M. G. Tomilin, *Interaction of Liquid Crystals with the Surface* (Politekhnika, St. Petersburg, 2001) [in Russian].

33. H. Haus, *Waves and Fields in Optoelectronics* (Prentice Hall, Englewood Cliffs, New Jersey, United States 1984; Mir, Moscow, 1988).

34. M. J. Stephen and J. P. Straley, Rev. Mod. Phys. **46**, 617 (1974).

35. W. H. De Jeu, W. A. P. Claassen, and A. M. J. Spruijt, Mol. Cryst. Liq. Cryst. **37**, 269 (1976).

36. V. Balakin, V. A. Bushuev, B. I. Mantsyzov, I. A. Ozheredov, E. V. Petrov, A. P. Shkurinov, P. Masselin, and G. Mouret, Phys. Rev. E: Stat., Nonlinear, Soft Matter Phys. **63**, 046 609 (2001).

37. H. J. Deuling, Mol. Cryst. Liq. Cryst. **19**, 123 (1972).

Translated by V. Astakhov